

Electronic Supplementary Information

One pot synthesis of environmentally friendly lignin nanoparticles with compressed liquid carbon dioxide as an antisolvent

Aye Aye Myint,^{‡a} Hun Wook Lee,^{‡a} Bumjoon Seo^a Won-Su Son,^a Junho Yoon,^a Tae Jun Yoon,^a
Hee Jeong Park,^a Jihyun Yu,^{a,b} Jeyong Yoon,^{a,b} and Youn-Woo Lee*^a

^aSchool of Chemical and Biological Engineering, College of Engineering and Institute of Chemical Processes (ICP), Seoul National University, 1 Gwanak-ro, Gwanak-gu, 151–744 Seoul, Republic of Korea.

^b World Class University (WCU) Program of Chemical Convergence for Energy & Environment (C2E2), School of Chemical and Biological Engineering, College of Engineering, Institute of Chemical Process (ICP), Asian Institute for Energy, Environment & Sustainability (AIEES), Seoul National University, 1 Gwanak-ro, Gwanak-gu, 151–742 Seoul, Republic of Korea.

* Corresponding author: Tel: +82-2-880-1883; Fax: +82-2-883-9124

E-mail address: ywlee@snu.ac.kr (Youn-Woo Lee)

[‡] These authors contributed equally to this work.

Table S1

Relative energy difference (RED) numbers for DMF and CO₂ with solubility sphere of lignin as a function of experimental temperatures (*T*) and pressures (*P*).

Solvent/Antisolvent	<i>T</i> (K)	<i>P</i> (MPa)	δ_d^a	δ_p^a	δ_h^a	$\delta_t^{a,b}$	<i>V</i> (cm ³ /mol)	$R_a^{a,c}$	RED ^d
DMF	280.2	15.0	17.7	13.8	11.5	25.2	76.1	9.655	0.705
	288.2	15.0	17.7	13.8	11.4	25.1	76.1	9.718	0.709
	298.2	15.0	17.6	13.8	11.3	25.0	76.3	9.874	0.721
	280.2	7.5	17.6	13.8	11.5	25.1	76.5	9.822	0.717
	288.2	7.5	17.6	13.8	11.4	25.1	76.5	9.883	0.721
	298.2	7.5	17.5	13.7	11.3	24.9	76.6	9.995	0.730
CO ₂	280.2	15.0	12.9	4.8	6.4	15.2	45.5	22.394	1.635
	288.2	15.0	12.3	4.7	6.5	14.7	47.3	23.443	1.711
	298.2	15.0	11.4	4.6	6.6	14.0	50.2	24.908	1.818
	280.2	7.5	12.1	4.7	6.6	14.6	48.0	23.736	1.733
	288.2	7.5	11.2	4.6	6.7	13.8	51.1	25.264	1.844
	298.2	7.5	9.6	4.3	7.1	12.6	57.8	28.015	2.045

^a The δ_d , δ_p , δ_h , δ_t and R_a are in units of MPa^{1/2}.

^b The total solubility parameter, $\delta_t = (\delta_d^2 + \delta_p^2 + \delta_h^2)^{1/2}$.

^c The solubility parameter distance, $R_a = [4(\delta_{d2} - \delta_{d1})^2 + (\delta_{p2} - \delta_{p1})^2 + (\delta_{h2} - \delta_{h1})^2]^{1/2}$.

^d Obtained with Hansen solubility parameters for lignin ($\delta_d = 15.6$, $\delta_p = 5.2$, $\delta_h = 5.8$, $\delta_t = 17.4$, $R_\theta = 13.7$, data fit = 0.990).⁵⁷

Table S2

Solubility parameter distances (R_a) for dissolving between DMF and CO₂ each other as a function of experimental temperatures (T) and pressures (P).

Solvent	T (K)	P (MPa)	δ_d^a	δ_p^a	δ_h^a	$\delta_t^{a,b}$	V (cm ³ /mol)	$R_a^{a,c}$
DMF	280.2	15.0	17.7	13.8	11.5	25.2	76.1	14.0
	288.2	15.0	17.7	13.8	11.4	25.1	76.1	14.9
	298.2	15.0	17.6	13.8	11.3	25.0	76.3	16.1
	280.2	7.5	17.6	13.8	11.5	25.1	76.5	15.0
	288.2	7.5	17.6	13.8	11.4	25.1	76.5	16.4
	298.2	7.5	17.5	13.7	11.3	24.9	76.6	18.9
CO ₂	280.2	15.0	12.9	4.8	6.4	15.2	45.5	14.0
	288.2	15.0	12.3	4.7	6.5	14.7	47.3	14.9
	298.2	15.0	11.4	4.6	6.6	14.0	50.2	16.1
	280.2	7.5	12.1	4.7	6.6	14.6	48.0	15.0
	288.2	7.5	11.2	4.6	6.7	13.8	51.1	16.4
	298.2	7.5	9.6	4.3	7.1	12.6	57.8	18.9

^a The δ_d , δ_p , δ_h , δ_t and R_a are in units of MPa^{1/2}.

^b The total solubility parameter, $\delta_t = (\delta_d^2 + \delta_p^2 + \delta_h^2)^{1/2}$.

^c The solubility parameter distance, $R_a = [4(\delta_{d2} - \delta_{d1})^2 + (\delta_{p2} - \delta_{p1})^2 + (\delta_{h2} - \delta_{h1})^2]^{1/2}$.

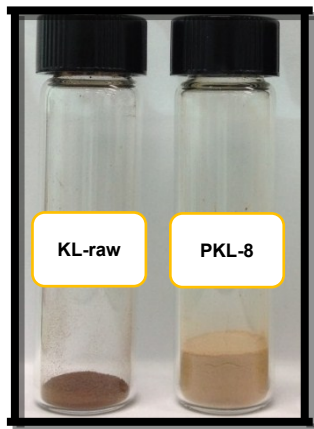


Fig. S1 The digital photographs of the lignin particles formed by the PCA process: PKL-8, and the unprocessed/raw lignin: KL-raw. The amounts are 100 mg for each sample.

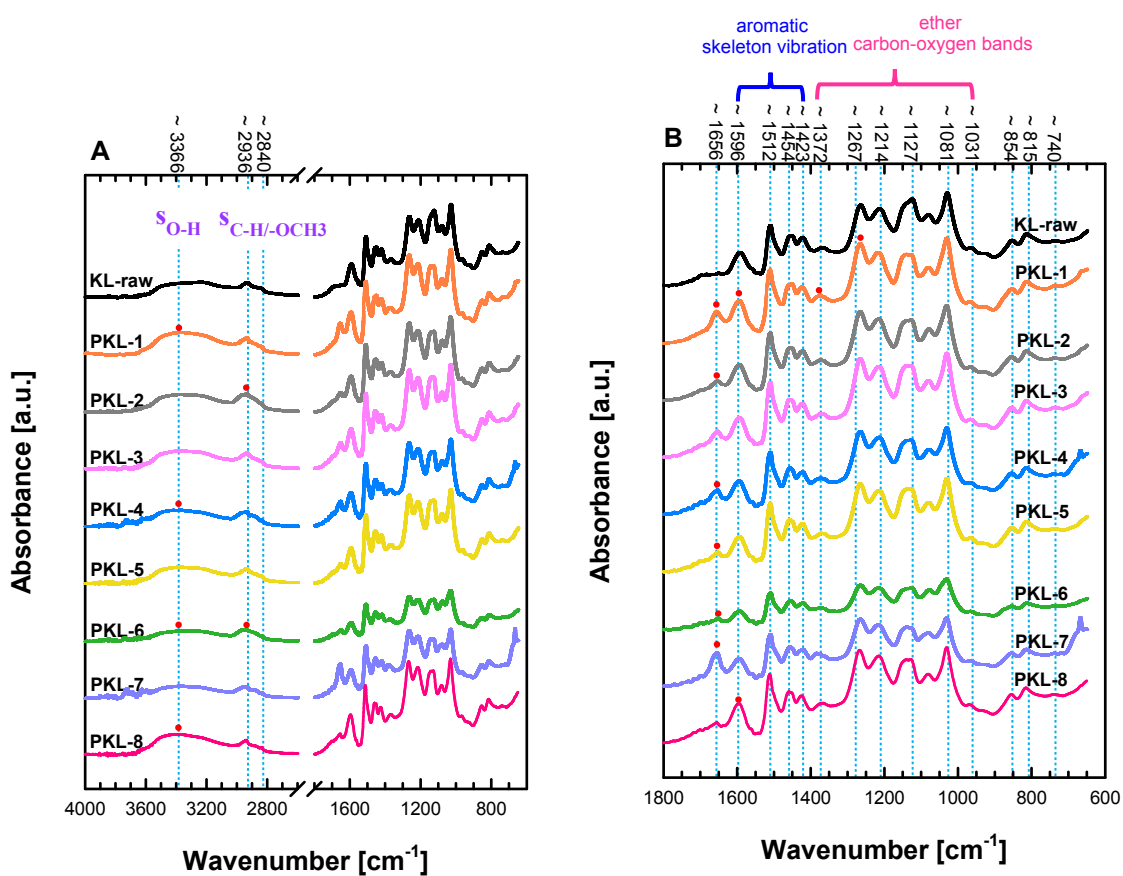


Fig. S2 ATR-FTIR spectra of the various processed lignin nanoparticles and raw lignin: the wavenumber ranges of 4000–600 cm^{-1} (A) and 1800–600 cm^{-1} (B), respectively. Red spheres indicate intense absorption peaks for the processed lignin samples in comparison to the raw lignin.

Table S3FTIR absorbance characteristics of the raw kraft lignin and various processed lignin nanoparticles using clCO_2 as an antisolvent.

Band origin with vibrational assignment	Wavenumber (cm^{-1})	The band intensity of normalized absorbance								
		KL-raw	PKL-1	PKL-2	PKL-3	PKL-4	PKL-5	PKL-6	PKL-7	PKL-8
O–H stretching of phenolic and aliphatic moieties	3380–3365	0.26	0.31	0.26	0.25	0.27	0.25	0.28	0.24	0.31
C–H stretching of $-\text{CH}_3$ / $-\text{CH}_2-$	2940–2936	0.25	0.23	0.27	0.22	0.24	0.23	0.31	0.23	0.23
C–H stretching of $-\text{OCH}_3$	2851–2840	0.16	0.12	0.13	0.12	0.11	0.12	0.15	0.11	0.12
Water associated lignin / conjugated C=O stretching	1657–1653	0.26	0.43	0.29	0.36	0.41	0.30	0.32	0.66	0.31
C–C stretching of aromatic skeleton	1596–1593	0.56	0.58	0.53	0.54	0.55	0.52	0.51	0.55	0.59
C–C stretching of aromatic skeleton	1512–1511	1.00	1.00	1.00	1.00	1.00	1.00	1.00	1.00	1.00
C–H deformation (asymmetric in $-\text{CH}_3$ and $-\text{CH}_2-$) and aromatic ring vibration	1459–1453	0.83	0.81	0.78	0.78	0.75	0.77	0.79	0.77	0.75
C–C stretching of aromatic skeleton plus C–H in plane deformation	1425–1422	0.80	0.77	0.74	0.72	0.69	0.71	0.73	0.72	0.69
O–H in-plane deformation in phenolic OH	1386–1367	0.63	0.65	0.60	0.59	0.59	0.57	0.61	0.54	0.59
C–O stretching plus guaiacyl unit (G)	1267–1266	1.34	1.36	1.31	1.31	1.33	1.29	1.21	1.29	1.34
C–OH (phenolic OH) stretching	1218–1214	1.27	1.24	1.20	1.21	1.24	1.19	1.13	1.18	1.26
aromatic C–H in-plane deformation of G	1140–1126	1.43	1.21	1.19	1.22	1.20	1.22	1.13	1.14	1.21
C–O deformation in secondary alcohols and aliphatic ether	1082–1079	1.18	1.04	1.06	1.02	1.05	1.02	1.09	1.03	1.00
aromatic C–H in-plane deformation G plus C–O deformation in primary alcohols plus conjugated C=O stretching	1033–1031	1.53	1.43	1.40	1.38	1.39	1.37	1.37	1.32	1.38
aromatic C–H out-of-plane deformation of G	856–854	0.76	0.74	0.50	0.60	0.67	0.50	0.64	0.65	0.71
aromatic C–H out-of-plane deformation of G	816–814	0.86	0.85	0.65	0.67	0.76	0.65	0.73	0.72	0.81
Condensation index (CI^a)		0.57	0.56	0.61	0.60	0.60	0.60	0.59	0.63	0.60

^a $CI = \text{sum of all minima between } 1500 \text{ and } 1050 \text{ cm}^{-1} / \text{sum of all maxima between } 1600 \text{ and } 1030 \text{ cm}^{-1}$.⁷⁹

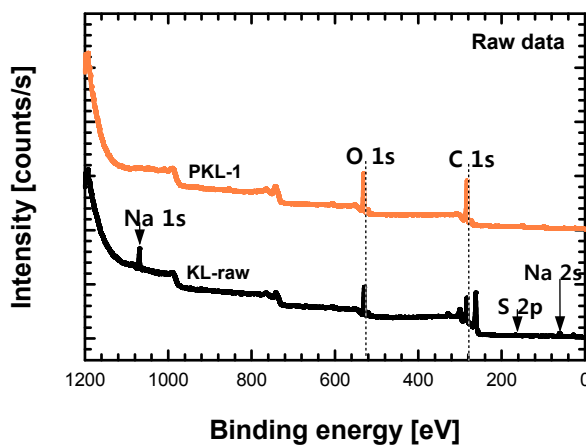


Fig. S3 XPS survey spectra for the raw lignin: KL-raw, and lignin nanoparticles: PKL-1.

Table S4

Elemental compositions of the surface of the raw lignin and processed lignin nanoparticles as calculated by XPS analysis.

Sample	Elemental composition (Atomic %)				C/O
	C	O	Na	S	
KL-raw	62.4	25.3	11.6	0.7	2.5
PKL-1	75.3	24.6	—	0.1	3.1

Table S5

Distribution of functional groups calculated on the basis of the deconvolution model of XPS C 1s and O 1s peaks.

Sample	Relative content of each component peak					
	C 1s (%)			O 1s (%)		
	C ₁ ^a	C ₂ ^b	C ₃ ^c	O ₁ ^d	O ₂ ^e	O ₃ ^f
KL-raw	74.18	2.46	23.37	60.23	39.77	—
PKL-1	68.50	26.67	4.81	—	37.77	62.23

^a the peak at 284.5 eV represents the C–C and C–H components.

^b the peak at 286.0–286.5 eV represents the C–O–C and C–OH components.

^c the peak at 288.5–288.9 eV represents O=C–OH component.

^d the peak at 530.5 eV represents the Ph=O, Ph–C=O and O–O components.

^e the peak at 531.5–531.8 eV represents the C=O and O=C–OH components.

^f the peak at 532.9 eV represents Ph–OH and C–O components.

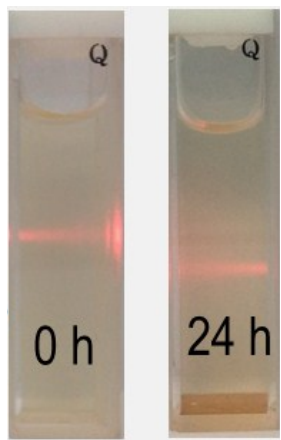


Fig. S4 The digital photographs for the lignin nanoparticles: PKL-1 were suspended in water at room temperature.

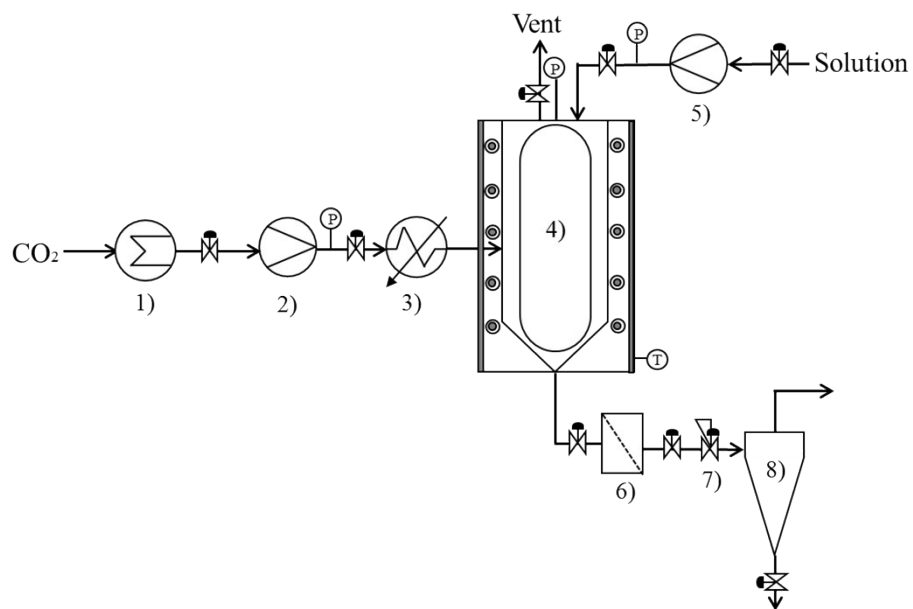


Fig. S5 A schematic diagram of the PCA experimental apparatus.

- 1) Cooler; 2) CO₂ pump; 3) Heater; 4) Precipitator; 5) Solution pump; 6) Filter; 7) Back pressure regulator; 8) Gas-liquid separator.